Pergamon

Int. J. Multiphase Flow Vol. 22, No. 3, pp. 461–472, 1996

0301-9322(95)00076-3
0301-9322/96 $15.00 + 0.00

THE INFLUENCE OF FLUID PROPERTIES AND INLET GEOMETRY ON FLOODING IN VERTICAL AND INCLINED TUBES

A. ZAPKE and D. G. KRÖGER

Department of Mechanical Engineering, University of Stellenbosch, Stellenbosch 7600, Republic of South Africa

(Received 12 March 1995; in revised form 15 November 1995)

Abstract—Flooding during adiabatic two-phase countercurrent flow in a vertical and 60° inclined (to the horizontal) 30 mm i.d. tube is investigated. Experiments are conducted with air, argon, helium, hydrogen, water, methanol, isopropanol and aqueous methanol solutions. An improved flooding correlation is proposed which accurately correlates the data. In the past, a number of proposed dimensionless groups often only succeeded in correlating their own data. The present correlation excellently correlates the data of three previous investigations. The findings clearly show that some flooding data had been misinterpreted in the past. The fluid densities have the strongest effect on the flooding gas velocity. The effect of the liquid viscosity is relatively stronger than that of the surface tension. Flooding is independent of the gas viscosity.

Key Words: gas–liquid flow, countercurrent flow, pressure drop, flooding, vertical flow, inclined flow

1. INTRODUCTION

During countercurrent two-phase flow, liquid flows down the tube wall under the action of gravity and gas, driven by, for example, a pressure difference, flows up the tube. This type of flow is found in air-cooled reflux condensers, such as dephlegmators or de-aerators, which are used in power generating cycles where steam drives a turbine. Flooding is also part of the safety analysis of nuclear reactors. Nuclear reactor design has been one of the driving forces behind two-phase flow and flooding studies. The flow rates and fluid properties encountered under hypothetical loss-of-coolant-accident conditions inside reactors differ from the low pressure steam conditions inside a dephlegmator, where steam at sub-atmospheric pressure is present. The above-mentioned differences and the fact that flooding fluid flow rates have not yet been correlated satisfactorily in terms of appropriate dimensionless groups, necessitate further experimental investigation for applications such as reflux condensers.

Flooding experiments were conducted with a sintered liquid inlet-type configuration in a vertical and 60° inclined (to the horizontal) tube. The flooding gas velocity was defined as the gas velocity at which the downflowing liquid begins to flow up past the liquid inlet sinter. Some investigators (Diehl & Koppany 1969; Chung *et al.* 1980) defined flooding in terms of a sharp increase in pressure drop across the test section. The question arises as to what extent the flooding fluid flow rates correspond for the above definitions, given the same type of sintered liquid inlet. The matter is clarified in section 3 with the aid of the experimental observations.

For a comprehensive survey on flooding literature, the reader may consult Bankoff & Lee (1986). McQuillan & Whalley (1985) compared existing flooding data and correlations for vertical flow. They presented a plot of 2762 flooding velocities in terms of the square root of the Wallis (1969) dimensionless superficial phase velocities

$$V_G^* = \left[\frac{\rho_G V_G^2}{gd(\rho_L - \rho_G)}\right]^{1/2} \quad [1]$$

$$V_L^* = \left[\frac{\rho_L V_L^2}{gd(\rho_L - \rho_G)}\right]^{1/2} \quad [2]$$

where d is the tube diameter, V_G and V_L are the gas and liquid superficial velocities, ρ_G and ρ_L are the gas and liquid densities and g is the gravitational acceleration. The data for the plot was obtained from different experimental configurations and the "scatter" illustrates the influence of the tube end geometries on flooding and that the dimensionless superficial velocities alone are not sufficient to correlate the data. Another possible cause for the "scatter" is the different flooding definitions used in the experimental investigations.

The aim of past flooding investigations was either to test the effect of the fluid properties on flooding or to identify the flooding mechanism and verify a corresponding theoretical model. Clift *et al.* (1966) approximately kept the liquid density and surface tension constant to test the effect of liquid viscosity. They found that the decrease in flooding gas velocity was of the order of 20% for a 70-fold increase in viscosity. Wallis (1969) conducted experiments and observed that the flooding gas velocity decreased with an increase in liquid viscosity. Experiments by Suzuki & Ueda (1977) showed that the flooding gas velocity had a tendency to increase with an increase in viscosity at a constant film thickness, but the trend was not so clear for the greater film thicknesses. Tests by Chung *et al.* (1980) with liquids having approximately equal densities and surface tensions, showed that the liquid viscosity had a small influence on flooding. They concluded that the change in liquid viscosity had to be 10- or 100-fold to have a significant effect on the flooding gas velocity. Further investigation by Chung *et al.* (1980) showed that surface tension had a stabilizing effect on flooding, i.e. the flooding velocity decreases with a decrease in surface tension. Experimental results of Suzuki & Ueda (1977) did not show a clear trend as far as the surface tension effect is concerned. Other investigators who tested the surface tension influence and who found the same trend as Chung *et al.* (1980) are English *et al.* (1963), Diehl & Koppany (1969) and Hewitt (1977). Kamei *et al.* (1954) found an opposite trend.

Flooding correlations in general indicate that the flooding gas velocity decreases with an increase in the gas density. The role of the gas viscosity has so far not been specifically investigated, but it has been included in some correlations to obtain certain dimensionless groups (e.g. Feind 1960).

Empirical flooding correlations are limited to the flow rates, fluid properties, tube geometry and inlet configurations they are based on. To overcome the limitations of empirical results, attempts have been made to model the flooding phenomenon theoretically. Mainly two kinds of mechanisms are suggested: (i) film flow models with shear as the primary momentum transfer mechanism (Taitel *et al.* 1982; Stephan & Mayinger 1992; Lacey & Dukler 1994); (ii) wave models and flow instabilities (Cetinbudaklar & Jameson 1969; Tien *et al.* 1980; Whalley & McQuillan 1985; Girard & Chang 1992).

The main objective of the work described in this paper is to determine the influence of the fluid properties, tube inclination and gas inlet configuration on flooding. Air, argon, hydrogen, helium, water, methanol, isopropanol and aqueous methanol solutions were used for this purpose.

2. EXPERIMENTAL APPARATUS

The properties of the fluids are shown in table 1. The fluid property range of each of the correlations recommended in this paper is given in table 2. The properties of the pure fluids were obtained from the literature. Samples of the aqueous methanol solutions were taken while conducting the experiments. The density, surface tension and viscosity were measured and compared to available information in the literature on properties of mixtures. The agreement was good. Because the methanol is more volatile with a water–methanol mixture, samples of the mixture were taken while conducting the tests, to monitor any possible changes in the fluid properties. A schematic of the flow loop is shown in figure 1. The transparent acrylic test section was mounted on a steel beam, which could be inclined at any position from horizontal to vertical. Compressed air was supplied by a 2 MN/m^2 reservoir and the flow gas was regulated with a pressure regulator. Argon, helium and hydrogen were supplied by 20 MN/m^2 pressurized bottles. The gas flow rate was regulated with a needle valve. The gas temperature could drop well below 0°C due to the expansion process at the needle valve. It was therefore passed through a 3/4 in. coiled copper tube. The copper tube was submerged in a water bath to heat the gas to approximately ambient temperature. Three orifice plates were used to obtain the desired range of metered gas flow. From the orifice plates the gas was introduced into the test section through the gas inlet device,

Table 1. Fluid properties, at ambient conditions ($p \approx 101325$ N/m^2; $T \approx 295$ K), used for the experimental investigation. The % indicates the percentage methanol (by volume) of an aqueous methanol solution

Fluid	Density (kg/m^3)	Viscosity $\times 10^6$ (kg/ms)	Surface tension $\times 10^3$ (N/m)
Air	1.196	18.230	—
Argon	1.650	22.390	—
Helium	1.653×10^{-1}	20.040	—
Hydrogen	8.325×10^{-2}	8.863	—
Water	998	958	72
Methanol	791	575	22
Isopropanol	784	2362	22
8% Methanol	987	1173	61
15% Methanol	977	1357	53
28% Methanol	961	1668	44
32% Methanol	955	1742	42
62% Methanol	903	1678	32

shown in figure 2(a). The gas entered the 127 mm i.d. tube through a ring chamber and 15 small equally spaced 20 mm long and 10 mm i.d. channels. The ring chamber was placed eccentric to the tube to obtain a uniform distribution through the small channels. A honeycomb section straightens the flow as it flows towards the sharp-edged flange. The sharp-edged flange could be replaced by a 137 mm long 7° tapered section to minimize the flow disturbance at the inlet to the 30 mm i.d. tube, which is shown in figure 2(b). The liquid was supplied by a constant level tank and recirculated with a pump, except the water which was drained to waste while testing. The liquid flow was monitored with a calibrated rotameter and introduced into the test section through a 180 mm long sintered section. The tube length between the gas inlet device and the sintered section was 2 m. The gas and liquid temperature was measured with copper–constantan thermocouples. The outlet of the return pipe was open to atmosphere and the test section pressure was therefore always just above the ambient pressure.

The flooding point was approached by slowly increasing the gas flow rate at a constant liquid flow rate. Liquid was carried above the sinter in the form of entrained droplets prior to the flooding point. Flooding, however, was said to commence when liquid started to flow up against the tube wall above the sintered section.

3. VISUAL OBSERVATIONS

The following paragraph describes the visual observations made during flooding in the vertical tube with the sharp-edged gas inlet. For detailed descriptions of the flow in the inclined tube with sharp-edged inlet and tubes (inclined and vertical) with the tapered inlet, the reader may consult Zapke (1994).

Without gas flow and at low gas flow rates small v-shaped waves were observed on the liquid film and the liquid drained from the 30 mm i.d. tube by accumulating in a "ring" of liquid on the face of the sudden contraction [figure 3(a)]. Droplets were separated from the "ring" by the action of gravity. As the gas flow rate was increased, a point was reached at which the "ring" of liquid suddenly was sucked into the 30 mm i.d. tube to form an oscillating disturbance. This was the onset of droplet entrainment into the gas stream. At this stage the entrained droplets did not reach the top of the test section above the liquid inlet and were deposited on the liquid film somewhere up the tube. The oscillating disturbance was annular in nature and occupied the bottom 10 cm of the test section tube. The liquid drained from the small diameter tube in curved strings of liquid,

Table 2. Fluid property ranges of the correlations presented in this paper

Equation	Gas density (kg/m^3)	Gas viscosity $\times 10^6$ (kg/ms)	Liquid density (kg/m^3)	Liquid viscosity $\times 10^3$ (kg/ms)	Surface tension $\times 10^3$ (N/m)
[4]	8.33×10^{-3}–1.65	8.86–22.39	784–998	0.575–2.497	22.8–72.4
[5]	8.33×10^{-3}–1.65	8.86–22.39	903–998	1.0–1.678	32.4–72.4
[6]	8.33×10^{-3}–1.65	8.86–22.39	998	1.0	72.4
[7]	1.65×10^{-1}–1.196	20.04–18.23	998	1.0	72.4

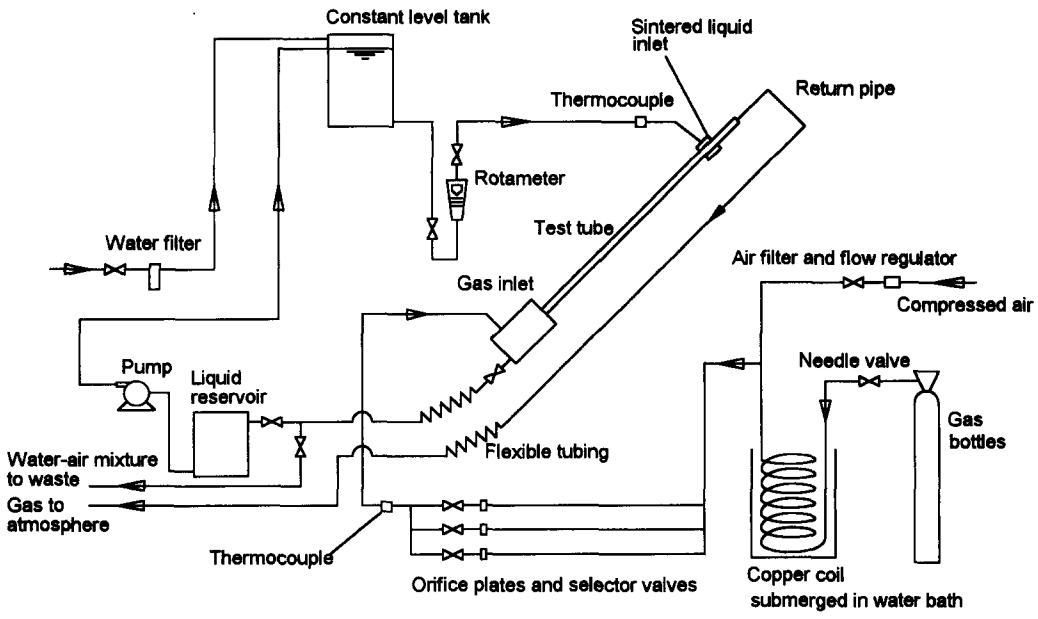

Figure 1. Schematic of the flow loop.

rotating around the tube axis, into the big tube as shown in figure 3(b). The above-described transition was very distinct. With a further increase in gas flow rate the disturbance remained at the bottom of the test section and eventually a gas velocity was reached at which a pulsating flow was created. The pulsating waves (formed at the gas inlet) initially did not reach the liquid inlet sinter and the liquid fell back to the bottom of the 30 mm i.d. tube, after the waves had slowed

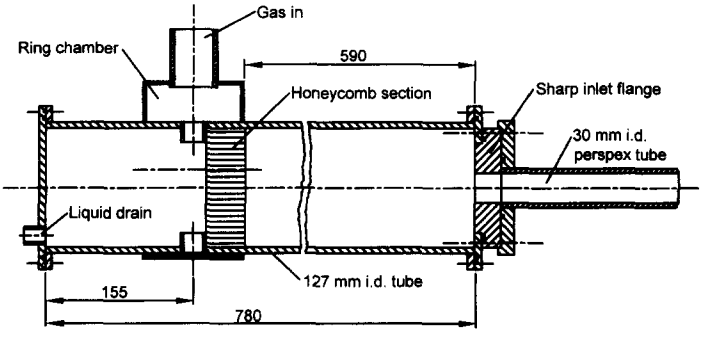

Figure 2(a). Detailed drawing of the gas inlet unit. Drawn to scale.

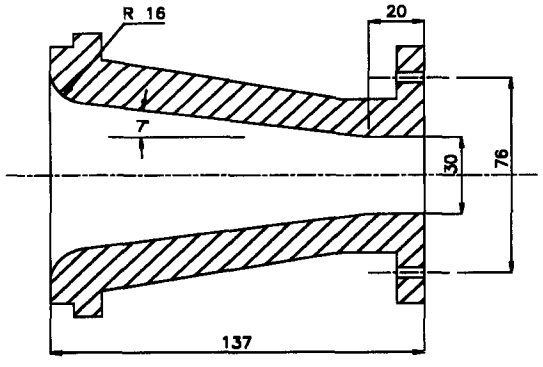

Figure 2(b). Tapered gas inlet flange for minimizing the entry effects during flooding.

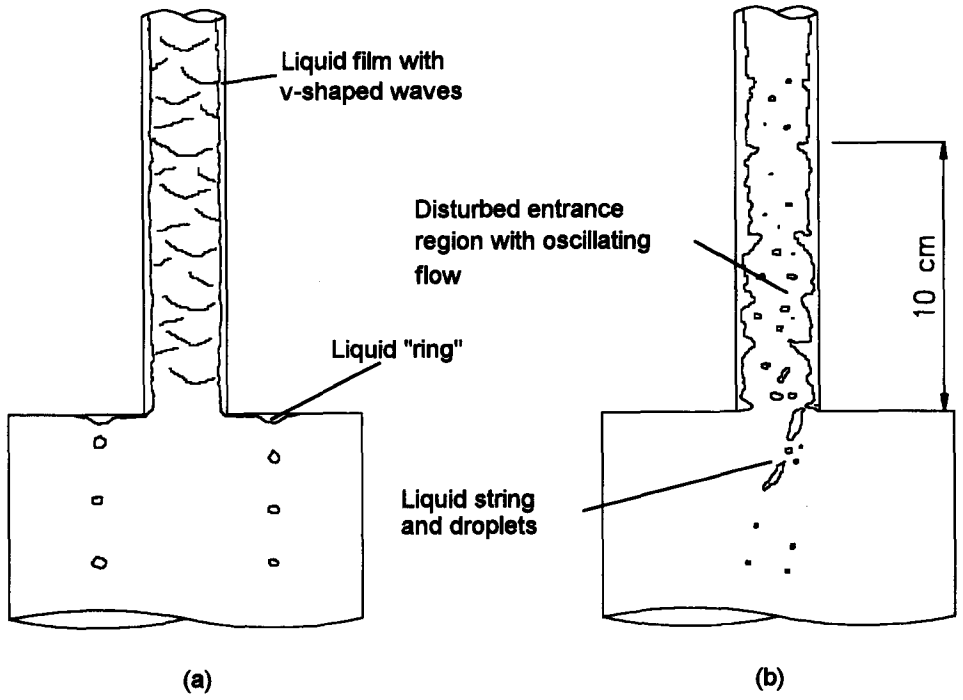

Figure 3(a). The liquid film is smooth and small v-shaped waves are observed. A liquid "ring" is formed on the face of the sudden contraction. (b) The liquid "ring" is sucked into the 30 mm i.d. tube and the flow at the gas entrance region is disturbed and oscillatory. Liquid is entrained.

down in speed somewhere up the tube below the liquid inlet. Once this pulsating type of flow occurred, the tube was filled with a churn-type flow up to the liquid inlet and liquid was transported up past the inlet sinter. Prior to this point, liquid was entrained along the entire tube below the liquid inlet and some of it was deposited against the tube wall above the liquid inlet to form a thin film that drained down the tube towards the sinter.

The pressure drop across the test section with the sharp gas inlet was measured while increasing the air flow rate until flooding was reached, to establish any possible differences between the two definitions (liquid feed and pressure drop definitions). The pressure drop increased gradually as the air flow rate was increased. At a certain air flow rate the tube started to fill up with a churn-type flow and while the gas flow was kept constant the pressure drop increased with time. Eventually liquid was carried above the feed point while the gas flow still remained unchanged. It can be concluded that the gas velocity at which the pressure starts to rise sharply and the gas velocity at

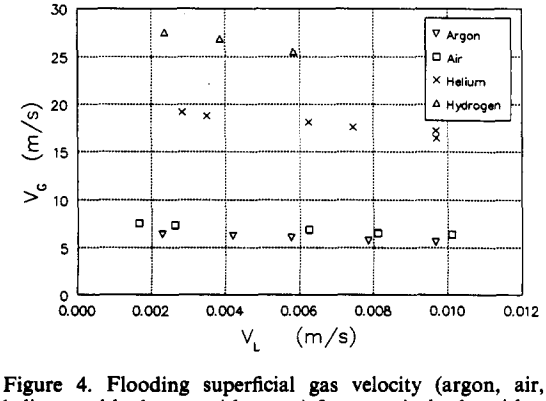

Figure 4. Flooding superficial gas velocity (argon, air, helium and hydrogen with water) for a vertical tube with a sharp-edged gas inlet.

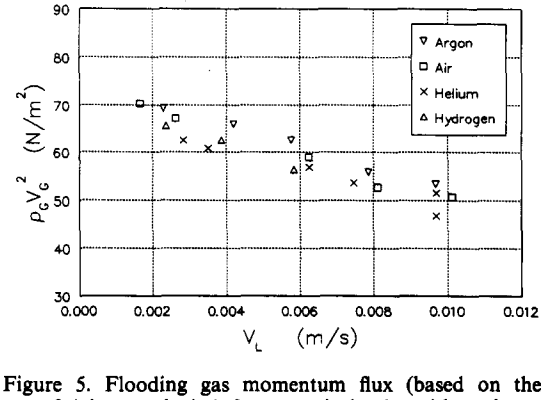

Figure 5. Flooding gas momentum flux (based on the superficial gas velocity) for a vertical tube with a sharp-edged gas inlet. Data obtained with argon, air, helium and hydrogen with water.

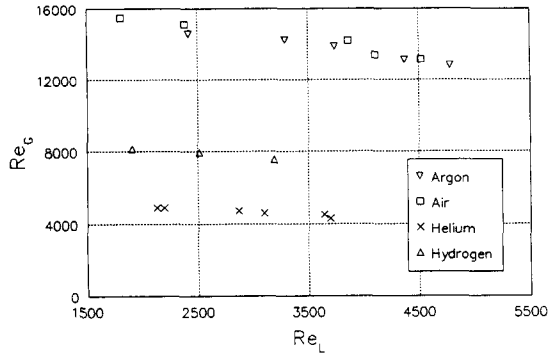

Figure 6. Flooding superficial gas Reynolds number for a vertical tube with a sharp-edged gas inlet. Data obtained with argon, air, helium and hydrogen with water.

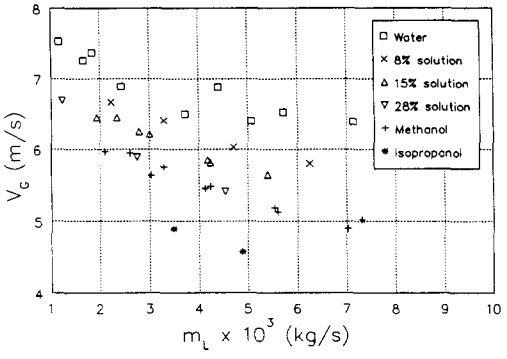

Figure 7. Superficial flooding gas velocities for a vertical tube with a sharp-edged gas inlet. Data obtained with water, aqueous methanol solutions, methanol and propanol with air.

which liquid is carried up past the liquid inlet are equal. The flooding results of a system with the definition "liquid flows up past the liquid feed" may therefore be compared to the flooding results obtained by measuring the fluid flow rates at the sudden increase in pressure. Both flooding velocities are equivalent in terms of the pressure drop characteristics of each particular system.

4. EXPERIMENTAL RESULTS

4.1. Sharp-edged gas inlet: vertical tube

The flooding superficial gas velocities obtained with the four gases and water are shown in figure 4. The results illustrate the wide range of velocities encountered due to the different gas densities. Figure 5 shows the flooding superficial gas momentum flux $\rho_G V_G^2$. The flooding superficial gas Reynolds numbers Re_G are plotted in figure 6. According to the plot, flooding does not occur at a certain Reynolds number at a given liquid flow rate. From figures 5 and 6 it can be concluded that flooding is independent of the gas Reynolds number and should be correlated in terms of dimensionless groups containing the superficial gas momentum flux.

Each of the different liquids together with air were used to investigate the influence of the liquid properties on flooding in the vertical tube with the sharp-edged gas inlet. The measured superficial flooding gas velocities plotted against the liquid mass flow rate m_L are shown in figure 7. Figure 8 is a plot of the same data in terms of $V_G^{*1/2}$ and $V_L^{*1/2}$. A certain trend is observed: as the percentage methanol increases, $V_G^{*1/2}$ decreases and the pure methanol and water dimensionless data are approximately equal. The data can be correlated with the Wallis-type equation (Wallis 1969)

$$V_G^{*1/2} + mV_L^{*1/2} = C \qquad [3]$$

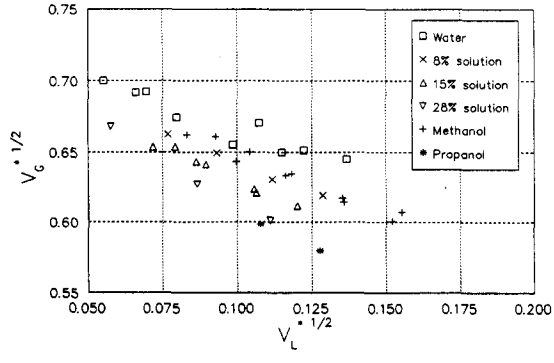

Figure 8. Dimensionless superficial flooding gas velocities for a vertical tube with a sharp-edged gas inlet. Data obtained with water, aqueous methanol solutions, methanol and propanol with air.

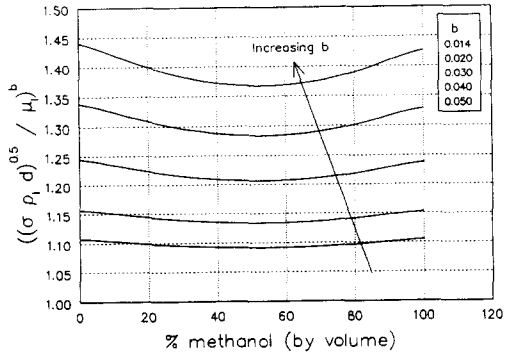

Figure 9. Plot of the dimensionless liquid property parameter Z_L (to the power of b) for the aqueous methanol solution as a function of the percentage methanol.

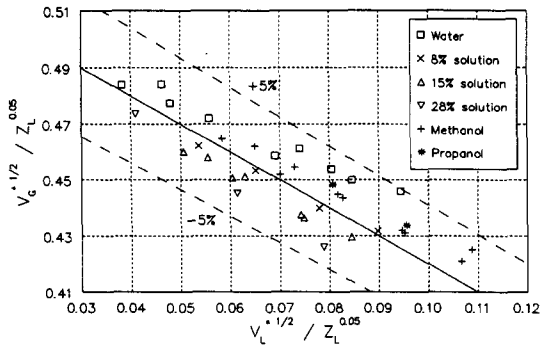

Figure 10. Flooding data for the vertical tube with a sharp-edged gas inlet in terms of the dimensionless groups $V_i^{*1/2}/Z_L^{0.05}$ (i = G, L). Data obtained with water, aqueous methanol solutions, methanol and propanol with air.

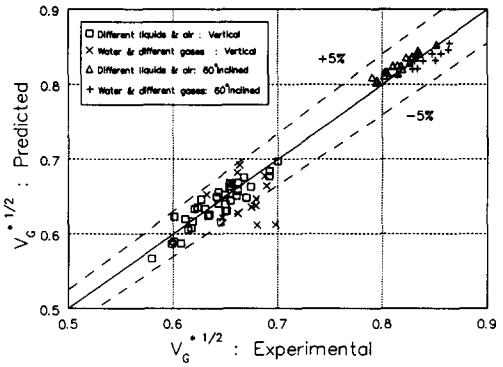

Figure 11. All the flooding data obtained with the sharp-edged gas inlet plotted as the predicted versus the experimental dimensionless superficial gas velocities.

where C is a function of the liquid properties and m is unity. A dimensionless combination of the aqueous methanol properties which exhibits a trend with a minimum, as the percentage alcohol is varied from 0 to 100%, is the parameter

$$Z_L = \frac{\sqrt{d\rho_L \sigma}}{\mu_L}$$

where μ_L is the liquid viscosity and σ is the surface tension. Figure 9 shows Z_L^b as a function of the percentage methanol for different values of b. b is an exponent which is to be determined empirically. Z_L^b is approximately equal at 0 and 100% methanol and goes through a minimum in between. A value of 0.05 for b correlates the data, including the isopropanol data. The resulting correlation is:

$$V_G^{*1/2} + V_L^{*1/2} = 0.52 Z_L^{0.05}. \quad [4]$$

The data obtained with the different liquids and air are plotted in figure 10 in terms of the dimensionless groups $V_i^{*1/2}/Z_L^{0.05}$ (i = G, L). The data lie inside a 10% band.

4.2. Sharp-edged gas inlet: inclined tube

No flooding data were obtained for the inclined tube with pure methanol and isopropanol. With these alcohols the tube flooded at the liquid inlet sinter before any pulsating flow was created from the bottom of the tube. In other words, the tube flooded at the liquid inlet while the flow below the sinter was still undisturbed. This was a different flow transition compared to the observations with all the other test runs (vertical liquid property tests and the gas–water tests with the sharp-edged gas inlet) and the results were therefore not considered for a flooding correlation.

The flooding data of the inclined tube was correlated in the same way as for the vertical tube, except that the dependence on the liquid properties μ_L and σ was less. The resulting correlation is:

$$V_G^{*1/2} + 0.6 V_L^{*1/2} = 0.8 Z_L^{0.014}. \quad [5]$$

The vertical and inclined flooding data, obtained with the different gases and liquids, are shown in figure 11 as predicted versus experimental dimensionless gas velocity.

4.3. Tapered gas inlet

Flooding tests were conducted with the four gases and water. As for the sharp-edged inlet data, the term $\rho_G V_G^2$ successfully correlates the gas flooding velocities, the gas viscosity playing no role in flooding. The vertical and inclined data are correlated as follows:

$$\text{Vertical flow:} \quad V_G^{*1/2} + 0.41 V_{L8}^{*1/2} = 0.86 \quad [6]$$

$$\text{Inclined flow:} \quad V_G^{*1/2} + 0.54 V_L^{*1/2} = 0.94. \quad [7]$$

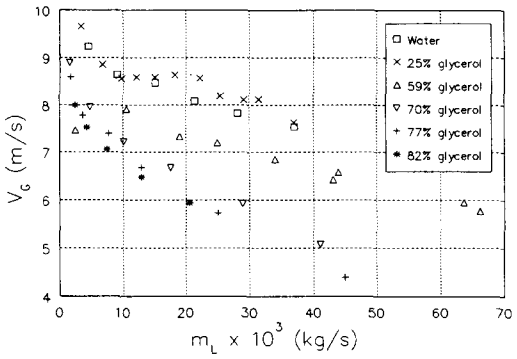

Figure 12(a). Flooding superficial velocities of the aqueous glycerol solutions tested by Clift *et al.* (1966) with a vertical tube with a bell-shaped gas inlet and a sintered liquid feed; $d = 0.03175$ m.

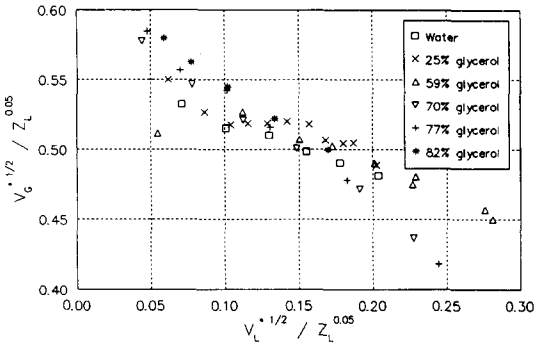

Figure 12(b). The flooding data of Clift *et al.* (1966) (figure 12(a)) plotted in terms of the proposed groups $V_i^{*1/2}/Z_L^{0.05}$.

5. EVALUATING THE VALIDITY OF THE GROUPS $V_i^{*1/2}/Z_L^{0.05}$ BY COMPARISON TO RESULTS OF PREVIOUS INVESTIGATIONS

5.1. *Clift* et al. *(1966)*

The flooding visual observations by Clift *et al.* (1966) (liquid bridging, chaotic flow pattern, liquid slugs being carried above the liquid inlet sinter) are similar to the present investigation's observations (vertical tube with sharp-edged gas inlet) and comparison is therefore justified. Figure 12(a) shows the superficial flooding gas velocities of the aqueous glycerol solutions, tested by Clift *et al.* (1966). The viscosity of the 25% glycerol solution is approximately twice the viscosity of water (the properties of the glycerol solutions are shown in table 3) and the density is 6% higher than the density of water. The flooding superficial gas velocities of the two above-mentioned liquids were found to be approximately equal. It is, however, wrong to conclude that the liquid viscosity has little or no effect because the liquid density primarily determines the gas flooding rate. In the above-mentioned case they counteract each other to yield equal flooding gas velocities. Figure 12(b) is a plot of the same data in terms of $V_i^{*1/2}/Z_L^{0.05}$. The data can be excellently correlated in terms of these dimensionless groups.

5.2. *Chung* et al. *(1980)*

The properties of the liquid used by Chung *et al.* (1980) are shown in table 4. Figure 13(a) shows the flooding results of the liquids selected to investigate the role of surface tension. The results were obtained with a sharp protruding gas inlet and the criterion for flooding was the appearance of a chaotic flow pattern or a sudden rise of gas pressure inside the test section. Note that the water and the surfynol solutions flood at equal gas velocities at high liquid flow rates. Only at the low liquid flow rates as the surfynol solutions flood at slightly lower gas velocities than water. The three above-mentioned liquids have equal densities. The silicon oil data lie below the water and surfynol solution data, primarily due its density of 820 kg/m^3, which is less than the density of the water and that of the solutions (1000 kg/m^3). Figure 13(b) is a plot of the data in terms of $V_i^{*1/2}/Z_L^{0.05}$. Figure 14(a) and (b) shows the results of their liquid viscosity experiments (flooding superficial velocities and dimensionless form, respectively). From figure 14(b) it can be seen that, except for

Table 3. Liquid properties of the liquids used by Clift *et al.* (1966) for flooding experiments with a vertical tube

% Glycerol	Viscosity $\times 10^3$ (kg/ms)	Density (kg/m^3)	Surface tension $\times 10^3$ (N/m)	$Z_L^{0.05}$ (—)
82%	82.5	1210	65.0	1.1591
77%	46.0	1200	65.8	1.1935
70%	23.4	1180	66.4	1.2343
59%	10.4	1150	68.0	1.2853
25%	2.18	1060	70.2	1.3880
Water	1.32	1000	72.0	1.4221

Table 4. Liquids tested by Chung *et al.* (1980). The liquid property parameter (Z_L) is calculated with $d = 0.0318$ m and $\rho_G = 1.2$ kg/m^3

Liquid	Viscosity × 10^3 (kg/ms)	Density (kg/m^3)	Surface tension × 10^3 (N/m)	$Z_L^{0.05}$ (—)
Water; 22°C	1.00	1000	72.7	1.4424
Water with surfynol SE 0.1% by weight; 20°C	1.00	1000	35.0	1.4163
Water with surfynol TG 0.1% by weight; 20°C	1.00	1000	28.0	1.4084
Silicon oil; 20°C	0.82	820	17.4	1.3987
Chevron white oil 3; 20°C	38.50	844.3	31.0	1.3144
Chevron white oil 5; 20°C	52.50	850.8	35.0	1.2983
Chevron white oil 9; 20°C	106.00	863.6	35.0	1.2549

a small deviation of the oil 3 data at low liquid flow rates, the data can be correlated in terms of these dimensionless groups. The dimensionless groups are therefore applicable at very high viscosities as well. Chung *et al.* (1980) wrongly concluded that the surface tension has a stronger effect on flooding than the liquid viscosity and that the change in viscosity has to be of the order of 10- to 100-fold to significantly effect the flooding gas velocity.

5.3. Stephan & Mayinger (1992)

Stephan & Mayinger (1992) conducted experiments with saturated Refrigerant 12 at high pressures. The fluid properties are shown in table 5. Flooding was investigated with a rectangular duct (0.068 × 0.02 m) with a sintered liquid inlet and a tapered vapour inlet. The radial void fraction distribution was measured with an optical fibre probe and no liquid bridging was observed. The flow pattern remained annular during the flooding process. Their observations differ from the chaotic flow observed in the present work, but it was still considered worthwhile to plot their data [figure 15(a)] in terms of $V_i^{*1/2}/Z_L^{0.05}$ [figure 15(b)]. What makes their combination of tests interesting is the high vapour densities and the liquid properties which yield approximately the same value for Z_L for all three system pressures tested. According to figure 15(b) the data can be correlated in terms of the dimensionless groups of that plot. A clear trend still exists (lowest dimensionless flooding gas velocities at $p/p_{crit} = 0.31$ and highest at $p/p_{crit} = 0.16$) but the percentage difference is small. The data lie inside an ≈6% band. The dimensionless groups $V_i^{*1/2}/Z_L^{0.05}$ are therefore applicable to correlate flooding data with minimized end effects and high gas densities and very low surface tensions.

6. CONCLUSIONS AND RECOMMENDATIONS

The results of the tests with the different gases prove that the flooding gas velocity is not dependent on the gas Reynolds number. The flooding superficial gas Reynolds number, for example, varies from ≈4000 (helium) to ≈16,000 (air) for the vertical tube with the sharp inlet. Flooding occurs at a specific gas momentum flux which in turn is related to the liquid flow rate,

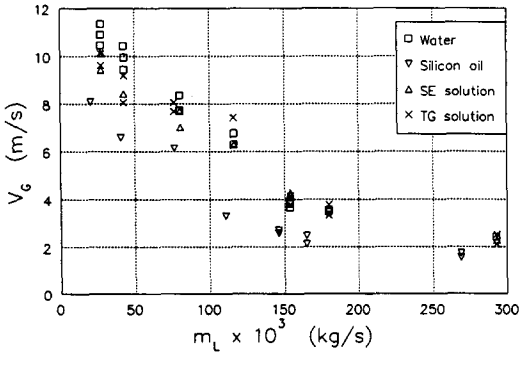

Figure 13(a). Flooding superficial velocities by Chung *et al.* (1980). Water, water with surfactants, silicon oil and air were used to investigate the effect of surface tension; vertical tube; $d = 0.0318$ m; sharp protruding gas inlet.

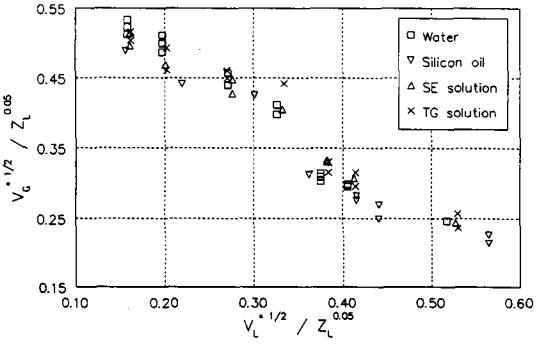

Figure 13(b). Data by Chung *et al.* (1980) (figure 13(a)) plotted in terms of the proposed groups $V_i^{*1/2}/Z_L^{0.05}$.

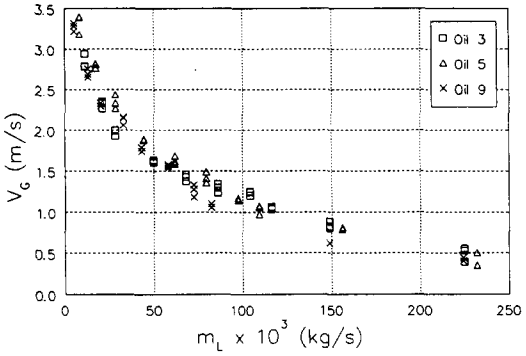

Figure 14(a). Flooding superficial velocities by Chung *et al.* (1980). Chevron white oil 3, 5 and 9 and air were used to investigate the effect of liquid viscosity; vertical tube; $d = 0.0318$ m; sharp protruding gas inlet.

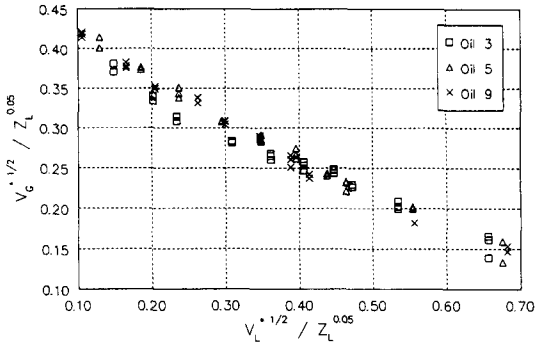

Figure 14(b). Data by Chung *et al.* (1980) (figure (14(a)) plotted in terms of the proposed groups $V_f^{*1/2}/Z_L^{0.05}$.

liquid properties and the system geometry. The gas viscosity does not play a role in the flooding process. The above-mentioned suggests that flooding is a drag phenomenon. The weight of the liquid is balanced by a drag force exerted by the upflowing gas. At low Reynolds numbers ($\mathrm{Re} \approx 10^3$ for a sphere) the drag force on solid submerged bodies is a function of the Reynolds nuber and the fluid dynamic head (ρV^2). At a certain Reynolds number ($\mathrm{Re} \approx 10^4$ for a sphere) the drag becomes independent of the Reynolds number and is proportional to the dynamic head only. Analogous to this the flooding process is independent of the gas Reynolds number.

To change one liquid property without affecting the other properties is one of the most problematic aspects of experimental flooding investigations. When investigating the role of a specific liquid property, a small variation in the remaining properties may have a considerable effect on the results, which can lead to incorrect interpretations. The dimensionless groups $V_G^{*1/2}$ and Z_L give a good indication of what the relative effects of the fluid properties on flooding are. Neglecting the liquid flow rate term in [4] (vertical flow) and solving for the flooding superficial gas velocity with $(\rho_L - \rho_G) \approx \rho_L$ the following is obtained:

$$V_G \propto \frac{d^{0.55} g^{0.5} \rho_L^{0.55} \sigma^{0.05}}{\rho_G^{0.5} \mu_L^{0.1}}. \qquad [8]$$

Equation [8] shows that the gas and liquid densities have the strongest effect on the gas flooding velocity. The surface tension has a very small stabilizing effect and the liquid viscosity influence on flooding is relatively stronger than the surface tension effect. The same arguments apply in the case of inclined flow, except that the surface tension and liquid viscosity influence on flooding is less than in the vertical case. The lower flooding gas velocities at higher liquid viscosities can also be explained in terms of the drag force idea. The film thickness is related to the liquid viscosity in countercurrent flow. [According to Feind (1960), the film thickness with and without gas flow does not differ significantly.] The available gas flow area is related to the film thickness. The thickness increases with an increase in liquid viscosity at a constant liquid flow rate, which in turn leads to a higher actual gas velocity and drag. Flooding will therefore occur at a smaller superficial gas velocity. Analogous to the above reasoning, the decrease in the flooding superficial gas velocity with an increase in liquid flow rate can be partly explained. The proposed correlations contain the tube diameter. The role of the diameter was not investigated and care must therefore be taken when applying the correlations to systems with different diameters. According to the drag force

Table 5. Liquids tested by Stephan & Mayinger (1992). The liquid property parameter (Z_L) is calculated with $d = 0.031$ m (hydraulic diameter)

System pressure (MN/m^2)	Liquid viscosity $\times 10^3$ (kg/ms)	Liquid density (kg/m^3)	Gas density (kg/m^3)	Surface tension $\times 10^3$ (N/m)	$Z_L^{0.05}$ (—)
0.67	0.210	1305	38.0	8.6	1.4874
1.0	0.180	1245	57.1	6.7	1.4878
1.3	0.150	1198	74.9	5.2	1.4905

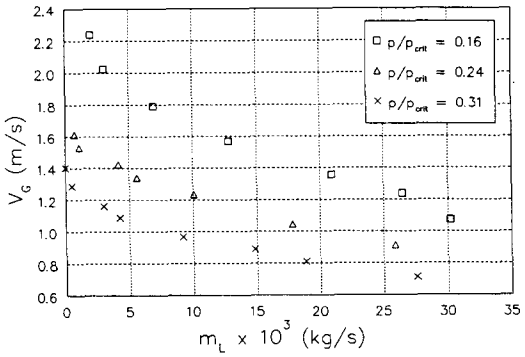

Figure 15(a). Superficial flooding gas velocities by Stephan & Mayinger (1992). Saturated Refrigerant 12 at three different pressures p was used as a working fluid in a rectangular duct (0.068 × 0.02 m) with a sintered liquid feed and a tapered vapour inlet (p_{crit} is the critical pressure of the fluid).

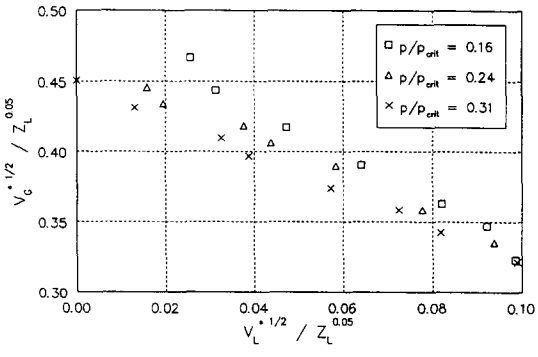

Figure 15(b). Data by Stephan & Mayinger (1980) (figure 15(a)) plotted in terms of the proposed groups $V_i^{*1/2}/Z_L^{0.05}$.

mechanism the diameter should not play a significant role. Some investigators found no diameter dependency (Girard & Chang 1992) while others did (Imura *et al.* 1977; Chung *et al.* 1980).

The sharp and tapered gas inlet data follows the expected trend of lower flooding gas velocities with the sharp inlet. The trend, however, is not necessarily due to the commonly suggested reason of the introduction of flow disturbances and the subsequent triggering of instabilities which leads to liquid upflow and flooding. A sudden contraction in flow area causes the gas flow to form a vena contracta. The gas velocity in the vena contracta is higher than elsewhere in the flow tube. The local higher velocity may be sufficient to cause a drag force on the liquid at the vena contracta to partially prevent it from leaving the flow tube, resulting in an accumulation of liquid in the tube. Flooding eventually occurs when the accumulating liquid reaches the inlet sinter. When the gas is introduced through a tapered inlet, the gas velocity is approximately equal in the entire two-phase region. Once the flooding gas velocity is reached, the flow direction of the liquid is reversed along the entire length of the flow tube. A more instantaneous flooding results, whereas in the case of the sharp gas inlet local "flooding" occurs at the bottom of the tube and progresses up the tube to the liquid inlet.

It is finally recommended that flooding data obtained with sharp-edged gas inlets and with configurations for minimized end effects should be correlated by

$$\frac{V_G^{*1/2}}{Z_L^b} + m\frac{V_L^{*1/2}}{Z_L^b} = E. \qquad [9]$$

The value of b depends on the tube inclination, E and m are dimensionless constants. Their values are determined by the tube end configuration and the tube inclination.

REFERENCES

Bankoff, S. G. & Lee, S. C. 1986 A critical review of the flooding literature. In *Multiphase Science and Technology* (Edited by Hewitt, G. F., Delhaye, J. M. & Zuber, N.), Vol. 2, Chap. 2, pp. 95–180. Hemisphere Publishing Corporation, New York.

Cetinbudaklar, A. G. & Jameson, G. J. 1969 The mechanism of flooding in vertical countercurrent two-phase flow. *Chem. Engng Sci.* **24,** 1669–1680.

Chung, K. S., Liu, C. P. & Tien, C. L. 1980 Flooding in two-phase countercurrent flows—II: Experimental investigation. *PhysicoChem. Hydrodynam.* **1,** 209–220.

Clift, R., Pritchard, C. & Nedderman, R. M. 1966 The effect of viscosity on the flooding conditions in wetted wall columns. *Chem. Engng Sci.* **21,** 87–95.

Diehl, J. E. & Koppany, C. R. 1969 Flooding velocity correlation for gas–liquid counterflow in vertical tubes. *Chem. Engng Prog. Symp. Ser.* **65,** 77–83.

English, K. G., Jones, W. T., Spillers, R. C. & Orr, V. 1963 Flooding in a vertical updraft partial condenser. *Chem. Engng Prog.* **59,** 51–53.

Feind, R. 1960 Falling liquid films with countercurrent air flow in vertical tubes. *VDI Forsch.* **481,** 5–35.

Girard, R. & Chang, J. S. 1992 Reflux condensation phenomena in single vertical tubes. *Int. J. Heat Mass Transfer* **35,** 2203–2218.

Hewitt, G. F. 1977 Influence of end conditions, tube inclination and physical properties on flooding in gas liquid flows. Harwell Report No. HTFS-RS 222 (1977). Quoted by Chung *et al.* (1980).

Imura, H., Kusuda, H. & Funatso, S. 1977 Flooding velocity in a counter-current annular two-phase flow. *Chem. Engng Sci.* **32,** 97–87.

Kamel, S., Onishi, J. & Okane, T. 1954 Flooding in a wetted wall tower. *Chem. Engng (Jap.)* **18,** 364–368. Quoted by Susuki & Ueda (1977).

Lacey, C. E. & Dukler, A. E. 1994 Flooding in vertical tubes—II. A film model for entry region flooding. *Int. J. Multiphase Flow* **20,** 235–247.

McQuillan, K. W. & Whalley, P. B. 1985 A comparison between flooding correlations and experimental flooding data for gas-liquid flow in vertical tubes. *Chem. Engng Sci.* **40,** 1425–1441.

Stephan, M. & Mayinger, F. 1992 Experimental and analytical study of countercurrent flow limitation in vertical gas/liquid flow. *Chem. Engng Technol.* **15,** 51–62.

Suzuki, S. & Ueda, T. 1977 Behaviour of liquid films and flooding in counter-current two-phase flow—part 1. Flow in circular tubes. *Int. J. Multiphase Flow* **3,** 517–532.

Taitel, Y., Barnea, D. & Dukler, A. E. 1982 A film model for the prediction of flooding and flow reversal for tubes. *Int. J. Multiphase Flow* **8,** 1–10.

Tien, C. L., Chung, K. S. & Liu, C. P. 1980 Flooding in two-phase counter-current flows—I: Analytical modelling. *PhysicoChem. Hydrodynam.* **1,** 195–207.

Wallis, G. B. 1969 *One-dimensional Two-phase Flow*, Chap. 11. pp. 336–345. McGraw–Hill, New York.

Whalley, P. B. & McQuillan, K. W. 1985 Flooding in two-phase flow: the effect of tube length and artificial wave injection. *PhysicoChem. Hydrodynam.* **6,** 3–21.

Zapke, A. 1994 Pressure gradient and flooding during two-phase countercurrent flow in inclined tubes. M. Engng thesis. University of Stellenbosch, Republic of South Africa.